Method for Analysing the Evolution with Magnetising Time of the Magnetic Barkhausen Noise Power Spectral Density

Amaia CASTELRUIZ, Ane MARTÍNEZ-DE-GUERENU, CEIT, San Sebastián, Spain
Fernando ARIZTI, CEIT and TECNUN (University of Navarra), San Sebastián, Spain

Abstract. In this paper, a new method for analysing the magnetic Barkhausen noise (MBN) measurements is presented. The proposed method analyses the power spectrum evolution with magnetising time of the MBN signal. The presented tool combines frequency and time domain information, avoiding the problems derived from the non-stationarity of the MBN signal, present in traditional frequency spectrum analysis.

The results obtained with the proposed method have a simple representation, similar to the root mean square (RMS) curves. Therefore, it allows a straightforward comparison of signals obtained with different samples. The tool is also simple to use, flexible and configurable, and it can be adapted to various analysis and applications.

As an example, the results obtained by the application of the method in a study of the influence of the quantisation of the magnetising signal on the MBN measurements are presented, and compared to the traditional RMS values. The information provided by the proposed method when applied to the whole power spectral density bandwidth is equivalent to the one given by the RMS values. However, when the method is applied to different frequency bands of the signal, it is capable of providing complementary information.

Introduction

The Magnetic Barkhausen Noise (MBN), which refers to discontinuous changes in magnetisation of a magnetic material when it is under the action of an external time varying magnetic field, is being used as an electromagnetic technique for non-destructive testing of stress [1-5] and microstructure [4-6]. In the literature, parameters corresponding to the time domain of the MBN signal are generally analysed, such as the Root Mean Square (RMS) curves, as well as their maximum peak amplitude [1-4] and position in terms of the magnetic field [1,4], or the number [2,3,6] and average amplitude of the detected pulses [2,6].

In the frequency domain, both the Fast Fourier Transform (FFT) and the power spectrum are frequently analysed [2,7-11]. However, care must be taken in the use of these tools. The MBN signal is not stationary, which means that its statistical properties vary along the hysteresis loop, that is, with the magnetising field applied. However, the MBN can be considered as statistically stationary in a small region around the coercive field, where the hysteresis loop is steepest and the properties of the signal remain invariant [12]. This implies that, unless considering only this small region around the coercive field, the FFT or the power spectrum of the MBN signal will vary with the magnetising field (or with

the equivalent magnetising time). For this reason, some authors have applied wavelet transforms [13] or spectrograms [14] for analysing the evolution with magnetising time of the frequency spectrum of the MBN signal. The main advantage of these tools is that they provide information of both time and frequency domain all at once. However, as a drawback, the result of applying these methods is three dimensional (time - frequency - amplitude). As an example, a spectrogram of a MBN signal is shown in Figure 1. Being the MBN a technique utilised for non-destructively testing stress or microstructural features, it is desirable to have tools that allow an easy comparison of the results obtained from different samples.

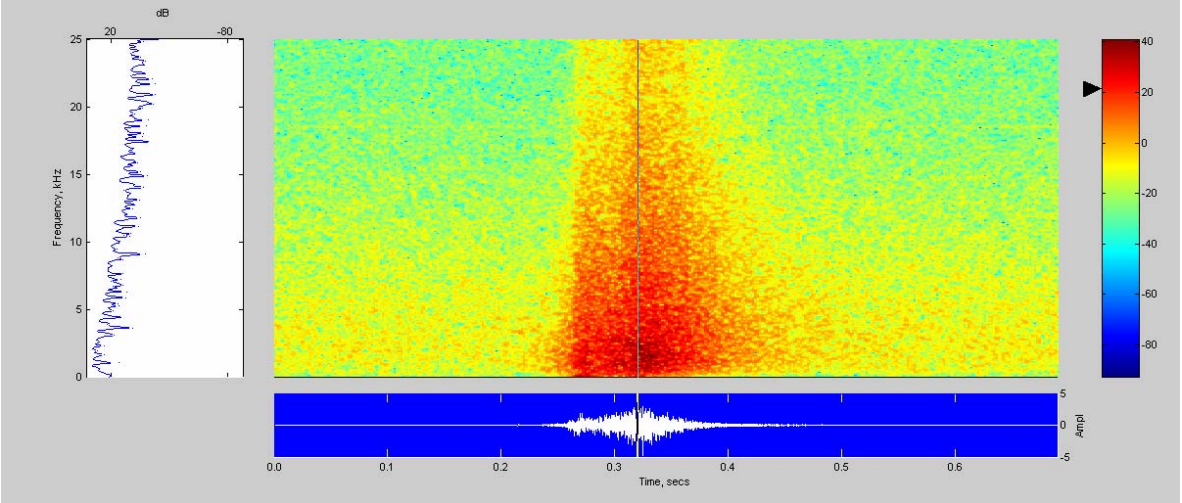

Figure 1. Example of a spectrogram of a MBN signal. The MBN signal is shown in the lower part of the image, and the power spectrum of the central region of the signal is shown on the left side of the image.

The method described in this paper presents a tool for analysing the power spectrum evolution with magnetising time of the MBN signal. The method developed gives information of both time and frequency domains, and it provides with a simple representation allowing a straightforward comparison of signals obtained with different samples. The tool is also simple to use, flexible and configurable as it can be adapted to various analysis and applications.

Method Description

The presented method is based on the calculation of the power spectral density (PSD) of the MBN signal. The PSD describes the distribution of the power of the signal with frequency [15]. If $f(t)$ represents the time series of the MBN signal, the spectral density $\Phi(\omega)$ of the signal is the square of the magnitude of the continuous Fourier transform of the signal, given by the following expression:

$$\Phi(\omega)=\left|\frac{1}{\sqrt{2\pi}}\int_{-\infty}^{\infty} f(t)\,e^{-i\omega t}dt\right|^2=\frac{F(\omega)\cdot F^*(\omega)}{2\pi}$$

where ω is the angular frequency (2π times the cyclic frequency) and $F(\omega)$ is the continuous Fourier transform of $f(t)$.

According to Parseval's theorem, the area under the PSD of a signal is equal to the area under the square of the magnitude of the signal, i.e. the power of the signal. As the power of a signal is also proportional to the square of its RMS curve, the area under the

PSD of a signal is proportional to the square of its RMS values. On the other hand, the area under a selected frequency band will represent the portion of the power of the signal contained in that particular band.

In this method, the PSD of successive time intervals of the MBN signal is calculated. Then, the area of the PSD under different frequency bands for each time interval is obtained and represented as a function of time. This way, the evolution with time of the power corresponding to the selected frequency bands can be studied.

A schematic representation of the method is shown in Figure 2. Firstly, the MBN signal is divided into time intervals, and the PSD of each interval is calculated. The length of each interval is small enough for the statistical properties of the signal to remain time-invariant within them. Then, a frequency band of the PSD is selected and the area under that band is calculated. The evolution of this area with time provides a curve similar in shape to the RMS curve of the time signal, which contains only the information regarding the selected frequency band.

The results of the process can be given in power units, representing the total power contained in the selected band. However, when several frequency bands of different lengths are analysed, wider bands might give higher values than the narrower bands, only because of the wider bandwidth considered. In these occasions it is interesting to calculate relative values, dividing the obtained power by the width of the selected band, and thus representing the average power in the selected band, independently of its width, in power units per Hz.

The method is parametrizable. Both the selected band and the number and length of intervals can be adjusted to each particular case. In the analysis presented in the next section, each interval was composed of 10000 samples, and the frequency bandwidth was divided into the following three bands:

- Low frequency band: 0 – 500 Hz
- Medium frequency band: 500 – 5000 Hz
- High frequency band: 5000 – 25000 Hz

Application of the proposed method

The presented method has been applied on data corresponding to a wider study on the influence of the quantisation of the excitation signal on MBN measurements [14].

Signals used for the excitation of MBN measurement systems are usually obtained by means of function generators or data acquisition (DAQ) boards. Both types of devices generate a quantised signal which consists of the reconstruction of the desired signal, using digital values. This quantised signal is represented as a set of rectangular pulses. The amplitude of the pulses is determined by the quantisation resolution (the number of bits used for representing the amplitude of the signal) and their width is given by the update rate or clock rate (the frequency at which new pulses are generated). This succession of pulses produces a reconstructed signal with an appearance of a step-like waveform.

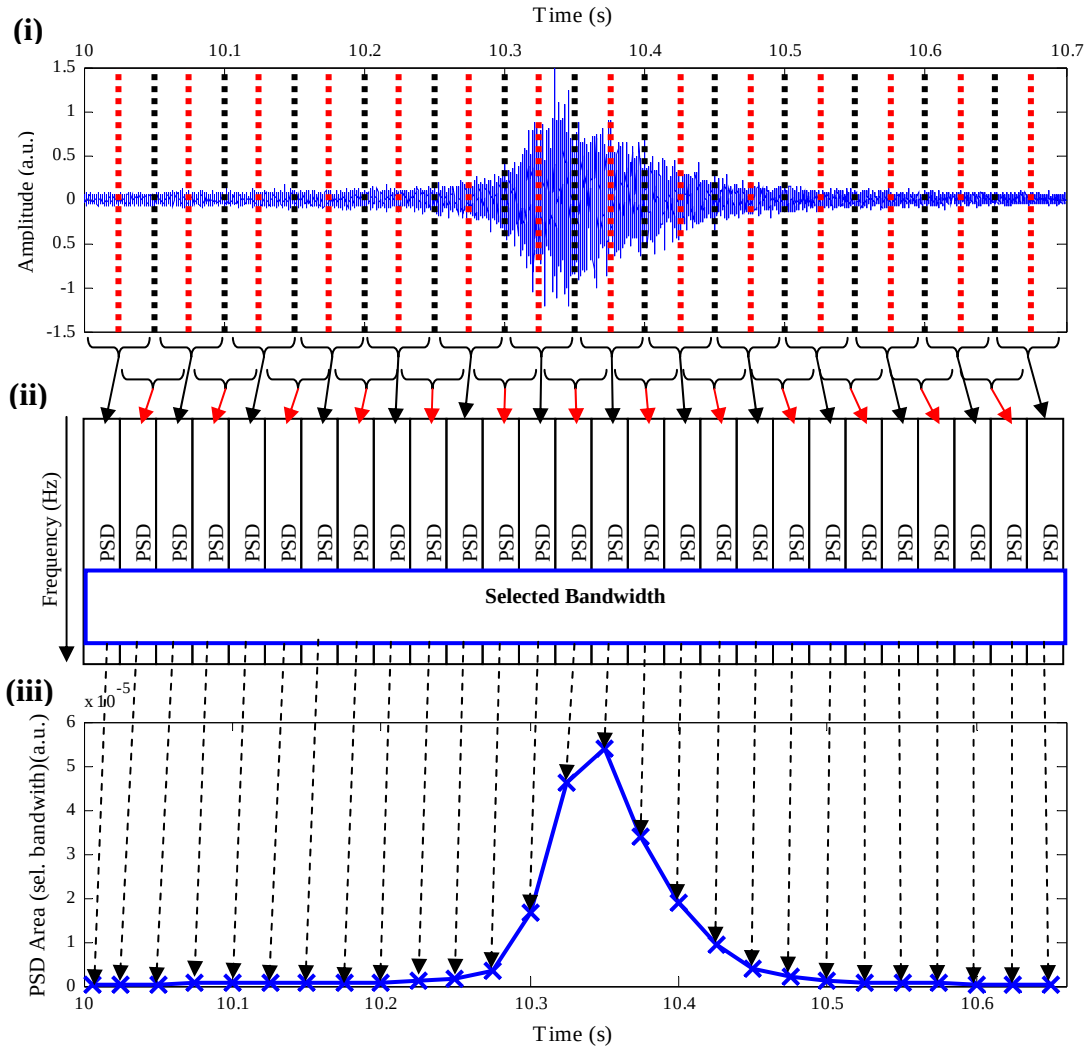

Figure 2. Schematic representation of the proposed method for analysing the power spectral density (PSD) of the MBN signal with magnetising time over different frequency ranges: i) MBN signal as a time series; ii) the PSDs calculated in each time interval as a function of frequency; iii) Areas of the PSD for the selected bandwidth as a function of the magnetising time.

Thus, the characteristics of the quantised signal depend on the quantisation resolution and on the update rate of the device. On the one hand, the resolution of the quantisation determines the amplitude of the pulses. As the resolution decreases, the difference between the pulses (the so-called steps) amplitude rises, and the reconstruction is more inaccurate. On the other hand, the update rate determines the number of pulses used in the reconstruction. As the update rate increases, more pulses are generated and the quantised signal is more similar to the ideal waveform being reconstructed. Furthermore, the quantisation effect, that is, the difference between the reconstructed and the original signal, can also be diminished low-filtering the quantised signal [15].

The influence of the quantisation features of the excitation on the resulting MBN signals is studied in the following sections. With that purpose, measurements were made using several excitation signals. The obtained MBN signals are analysed using traditional methods, such as the RMS, and the method proposed in this work.

Experimental Procedure

Sinusoidal, triangular and trapezoidal excitation waveforms with different quantisation characteristics were applied to obtain MBN signals, in order to study the influence of both the quantisation features and the shape of the waveform on MBN measurements.

Data were obtained with a measurement system developed in the author's laboratory, shown in Figure 3. As has been mentioned, several excitation signals with different quantisation characteristics were generated, using an analogue output of a National Instruments PCI-6014 multifunction DAQ card with 16-bit resolution in a range of 20 V and a maximum update rate of 10 kS/s. Output waveforms with 12-bit and 14-bit resolution were programmed and fed through the power amplifier to a 200 turn coil wound around a U-shaped magnetic core. Additionally, to obtain another set of exciting signals, these 12-bit and 14-bit waveforms were low-pass filtered (10 Hz cutoff frequency and -40 dB/decade attenuation), in order to diminish the influence of the quantised steps, before being fed to the power amplifier.

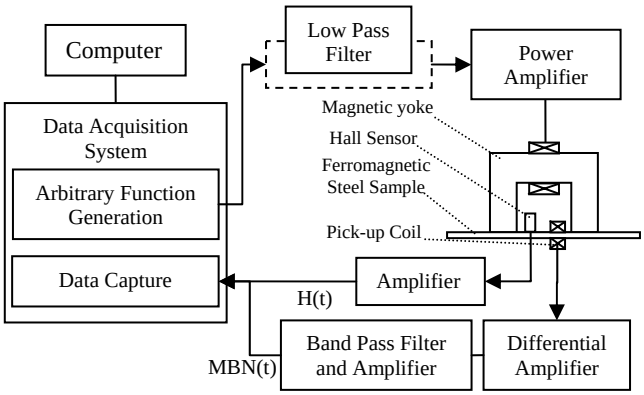

Figure 3. Schematic diagram of experimental setup for MBN measurements.

Sinusoidal, triangular and trapezoidal excitation waveforms of 0.1 Hz were used. The maximum amplitude of all the waveforms applied was ±2 V, which generated a field of ±4100 A/m, enough to obtain complete magnetic saturation of the samples. The slope of the trapezoidal waveform was chosen in such a way that it was equal to the maximum slope of the sinusoidal waveform. In all cases, the 12-bit resolution excitations had a minimum step amplitude of 0.97 mV, whereas in the case of 14-bit resolution signals their minimum amplitude was 0.3 mV.

MBN measurements were acquired for each of the excitation waveforms, demagnetising the samples at the test frequency before each measurement. The MBN was detected with a small 50 turn coil encircling the samples. The signal at the output of the differential pre-amplifier was further amplified and band pass filtered in the range 0.1 to 25 kHz. The tangential magnetic field strength was determined by a Hall probe placed at the surface of the steel samples. The sampling rate for both signals was 50 kHz. The signals picked up from both sensors were acquired by a DAQ system, stored in a personal computer and post-processed using MATLAB software.

Data were obtained from two samples of extra low carbon steel, 0.3 mm thick, 12.5 mm wide and 20 cm long. Sample 1 ("S1") was industrially cold rolled and sample 2 ("S2") was cold rolled and isothermally annealed for 4.8 h at 500ºC in a laboratory in order to decrease the dislocation density by recovery mechanisms [16].

Results and discussion

As has been mentioned, the effect of the described excitation signals on the MBN measurements is studied in this section by analysing the RMS values as well as the evolution of the PSD with time in several frequency bands applying the proposed method (Section 2).

- *RMS values*

Figure 4 shows the effect of the signal quantisation on the RMS curves of the MBN signals obtained with trapezoidal excitation waveforms for samples S1 and S2. For both samples, the RMS profile corresponding to the 12-bit unfiltered excitation shows higher amplitude than in the case of the 14-bit resolution unfiltered signal.

As the Barkhausen emission is proportional to the rate of change of the applied magnetic field with time (dH/dt) [17], these results are coherent because, as has been indicated, the applied 12-bit resolution signals had steps of amplitude three times higher than the ones corresponding to the 14-bit resolution signals. Moreover, Figure 4 shows a reduction in the gap between the 12-bit and 14-bit resolution signals when a low-pass filter is applied to the magnetisation signals. Comparing the results from both samples, it is observed that, for any of the excitations used, due to the reduction in the dislocation density produced by the recovery processes [16], after annealing the cold rolled sample, the amplitude of the MBN increases and the peak position shifts to lower magnetic field amplitudes [18]. This effect has been obtained for the three types of waveform used in the experiments.

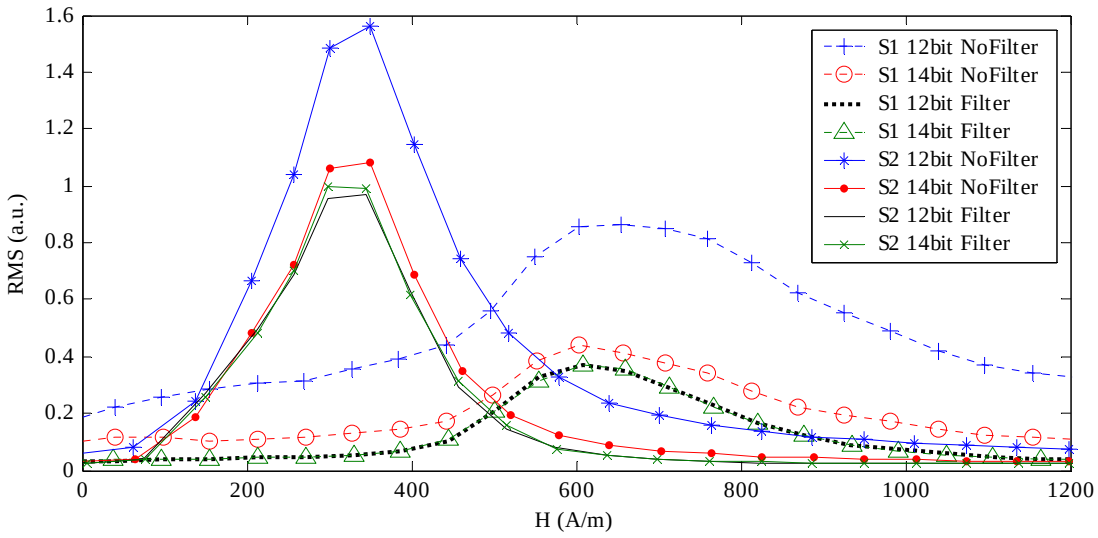

Figure 4. RMS profiles of the MBN signal obtained with cold rolled (S1) and cold rolled and annealed (S2) samples with 12-bit and 14-bit resolution unfiltered and filtered trapezoidal waveforms.

The comparison of the RMS profiles obtained with different 14-bit resolution unfiltered excitation signals is shown in Figure 5. It is important to note that, as has already been mentioned, the slope of the trapezoidal waveform was made equal to the maximum slope of the sinusoidal signal. This explains why both curves have very similar amplitudes. On the other hand, since all the waveforms had the same maximum amplitude, the triangular waveform had a lower slope. Therefore, the curve obtained for the triangular excitation presents slightly lower amplitude than the others.

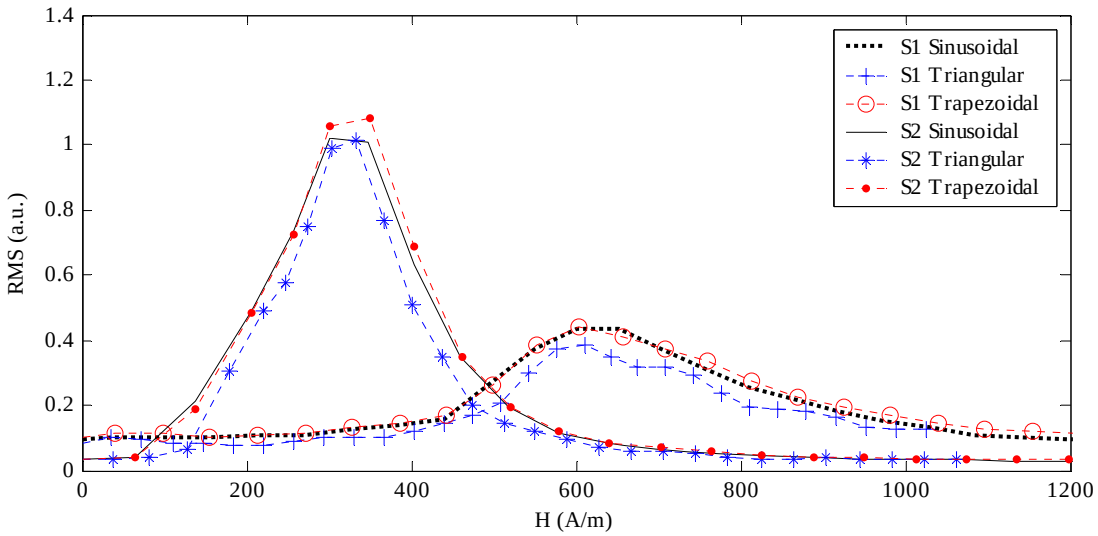

Figure 5. RMS profile curves obtained for samples S1 and S2 with a 14-bit resolution unfiltered sinusoidal, triangular and trapezoidal excitation signals.

- *Area under the power spectral density (PSD)*

The results of the application of the proposed method on the data corresponding to the different sinusoidal excitation signals are shown in Figure 6. The evolution with the magnetising field of the area under the PSD, for each of the selected frequency bands is represented in each Figure. Figure 6-a shows the PSD under the total bandwidth (TB) and Figures 6-b, 6-c and 6-d represent the PSD under the frequency bands defined in Section 1 as low band (LB), medium band (MB) and high band (HB), respectively. The presented values are normalised, respectively, by the width of each selected band, as has been explained in Section 2. It is observed that different power distributions are obtained for each excitation signal.

As can be seen, in the low frequency band (from 0 to 500 Hz) (Figure 6-b), the curves obtained for both S1 and S2 samples with the 12-bit sinusoidal unfiltered excitation signal have more than twice the power of the 14-bit unfiltered excitation signals. The latter is also more than five times higher than the signals corresponding to the filtered 12 and 14-bit excitation signals. In the medium frequency band (from 500 Hz to 5 kHz) (Figure 6-c), the dissimilarities between the curves corresponding to different excitation signals are smaller. This is especially notorious between the 14-bit unfiltered and the 12 and 14-bit filtered excitation signals, which are all very similar in amplitude. In the case of the high frequency band (from 5 to 25 kHz) (Figure 6-d), it is observed that practically no differences exist between the distinct excitation signals used, as for each sample the PSD curves obtained in this frequency range are practically the same.

These results show that the effect of the quantisation of the magnetising signal is highest in the lowest frequency ranges. The curves obtained with the 12 and 14-bit filtered excitation signals show nearly no quantisation effect. At medium frequencies, the signal obtained for the 14-bit unfiltered excitation signal, in which the quantisation effect is not very important, becomes very similar to the 12 and 14-bit filtered excitation curves. However, the curves obtained with the 12-bit unfiltered excitation signal, in which the quantisation effect is strongest, still show more power in these medium frequencies. It is observed that these curves become similar to the rest of the curves when the highest frequencies are analysed.

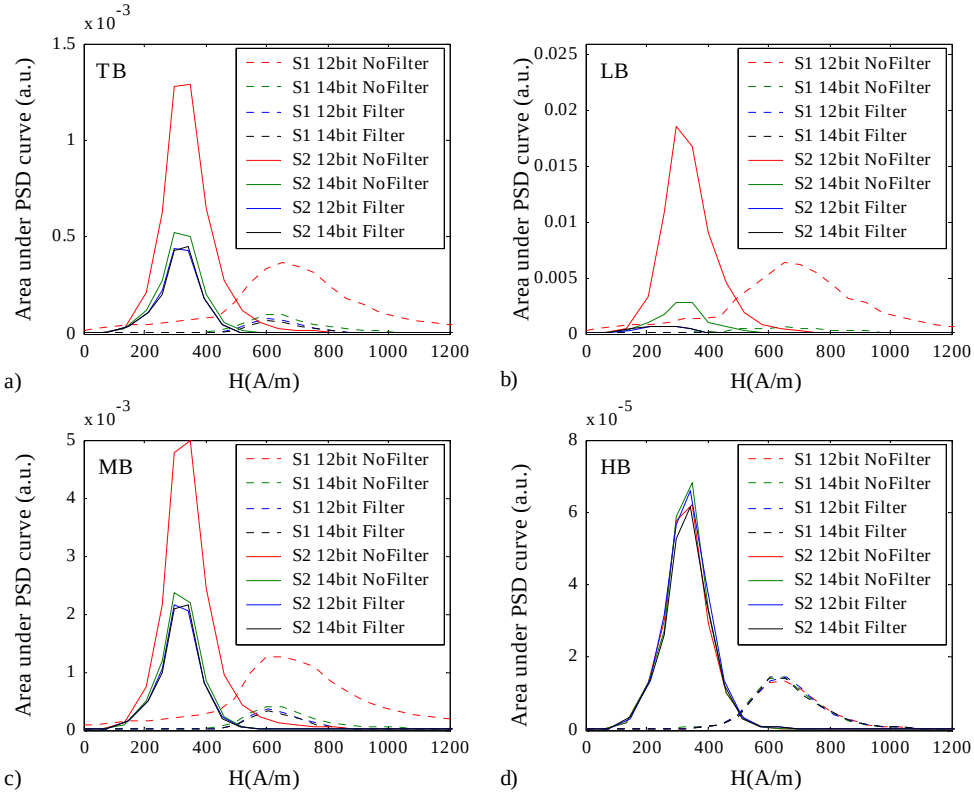

Figure 6. Evolution of the area under the PSD curves for samples S1 and S2, and for 12 and 14-bit resolution, unfiltered and filtered sinusoidal excitation signals. Figure 6-a shows the curves corresponding to the total bandwidth (TB) of the PSD of the signal. Figures 6-b, 6-c and 6-d show, respectively, the values corresponding to the low (LB), medium (MB) and high (HB) frequency bands. Note the normalisation of the values by the width of each selected band.

Thus, from these results it can be concluded that the higher the quantisation effect in the excitation signal the higher the power of the MBN signal at the lowest frequencies of the spectrum, and that the power due to the quantisation of the excitation reaches higher frequency ranges as the quantisation resolution is lowered. On the other hand, the power present in the highest frequency band of the spectrum, although it is much lower in amplitude than the power existing in the rest of the bands, does not show any effect of the quantisation characteristics of the magnetising signal. And hence, the information contained in that frequency band can be attributed only to be related to the characteristics of the sample measured, with no additional effect of the quantisation of the exciting or magnetising signal.

- *Resolution of the studied methods*

In order to further analyse the resolution of the PSD curves obtained in the different frequency bands studied, in terms of the differences found between the two steel samples measured, a so-called “S2/S1 ratio” was defined as the ratio between the maximum amplitude peaks corresponding to the curves obtained for samples S2 and S1. Figure 7 shows the S2/S1 ratio found for the PSD curves under the low, medium and high frequency bands and for the total bandwidth, as well as the same ratio calculated with the maximum amplitudes of the RMS curves, for comparison. The ratios in each of the frequency bands corresponding to the four types of quantisation signals used for sinusoidal, triangular and trapezoidal waveform types are represented.

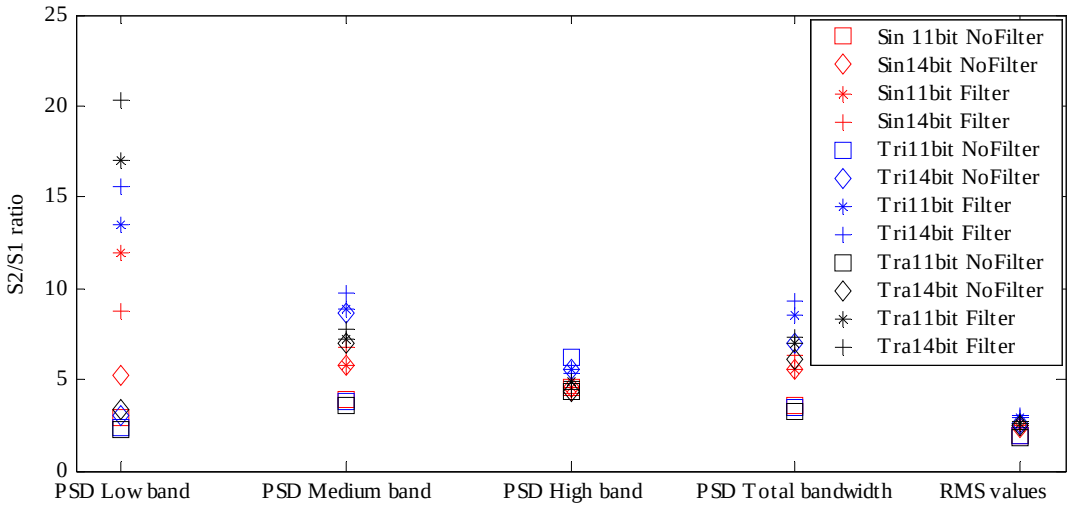

Figure 7. Ratio between the maximum amplitude peaks corresponding to the curves obtained for samples S2 and S1 for the PSD areas under the low, medium and high bands, and for the total bandwidth, and for the RMS curves. The values correspond to the 12 and 14-bit resolution, both unfiltered and filtered, sinusoidal, triangular and trapezoidal excitation signals.

It is observed that the S2/S1 ratio corresponding to any of the PSD areas calculated by the proposed method shows higher values than the ratio corresponding to the RMS curves. In the case of the data corresponding to the whole bandwidth of the PSD, the values are higher than the ones obtained with the RMS curves because, as has been indicated in Section 2, the area under the PSD is proportional to the square of the RMS values.

It should be noted that S2/S1 ratio values present a large dispersion in the low frequency band. This effect can be attributed to the fact that the values of the curves obtained for sample S1 corresponding to the filtered excitations are extremely low in amplitude, which increases the relative error of these measurements. On the other hand, as explained in previous subsections, the quantisation effect of the excitation signal is more significant in the lowest frequencies, both in the low and medium frequency ranges. Thus, differences are found between the areas under the PSDs in these frequency ranges of the 12-bit unfiltered excitation signals, for which the quantisation resolution is the lowest and therefore the quantisation effect is the highest, and the 14-bit unfiltered excitation signals, for which the quantisation resolution is better.

As has been pointed out, the information provided by the high frequency band is independent of the excitation properties such as waveform type and its quantisation characteristics, in such a way that it depends only on the slope of the magnetising field applied, dH/dt, and on the material's microstructure. For that reason, the resulting values show very little dispersion between themselves. It must also be noted that the amplitude of the area under the PSD in these frequencies is very low, because it is affected by the attenuation exerted by the material at high frequencies.

- *Relation between the RMS values and the area under the PSD curve*

As mentioned, the area under the PSD curve, if the complete bandwidth of the MBN signal is considered, corresponds to the square of the RMS values. The relation between the square of the RMS values and the area under the PSD curve, calculated by the proposed method selecting the whole bandwidth of the signal, is represented in Figure 8. The data corresponding to the MBN signals obtained for samples S1 and S2, for the 12 and 14-bit, both unfiltered and filtered, sinusoidal excitation signals are included in the Figure. The linear correlation obtained between these parameters, which is satisfied for both samples irrespective of the excitation waveform used, proves that both parameters are proportional.

Hence, when the whole bandwidth of the signal is selected, the described method provides the same type of information as the RMS curves. However, once the bandwidth is divided into several ranges, information concerning the frequency domain, impossible to achieve from the RMS curves is obtained.

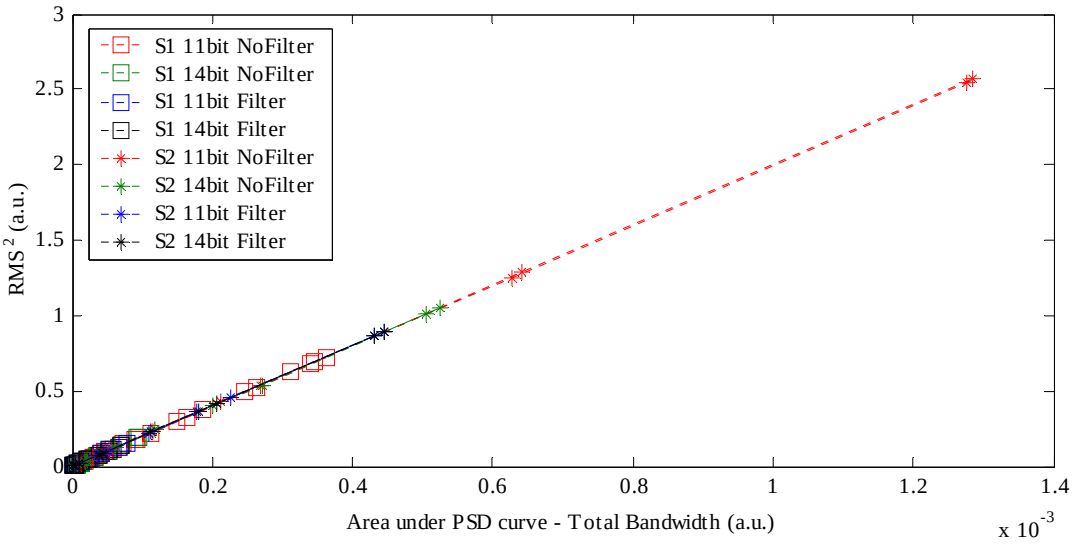

Figure 8. Correlation between the square RMS values and the area under the complete PSD obtained for samples S1 and S2 and 12 and 14-bit resolution, both unfiltered and filtered sinusoidal excitation signals.

Conclusions

The designed method allows combining the simplicity of the use of RMS curves with the information regarding the frequency distribution of the power of the signal. It has been proved that it is useful when comparing the power distributions in the frequency domain of various samples.

The method is easy to use, flexible and configurable, and the resulting curves are as easily parametrizable as RMS curves.

The method has been applied to study the influence of the quantisation of the excitation signal in MBN measurements. The information provided by the method when applied to the whole power spectral density bandwidth is equivalent to the one given by the RMS values. Nevertheless, when the method is applied to different frequency bands of the signal, it is capable of providing complementary information.

Acknowledgments

The authors would like to thank the Basque Government for partially funding this research project.

References

[1] V. Moorthy, B.A. Shaw, S. Day, "Evaluation of applied and residual stresses in case-carburised En36 steel subjected to bending using the magnetic Barkhausen emission technique", *Acta Materialia*, 52, 1927-1936, 2004.

[2] C. Jagadish, L. Clapham, D.L. Atherton, "Influence of Uniaxial Elastic Stress on Power Spectrum and Pulse Height Distribution of Surface Barkhausen Noise in Pipeline Steel", *IEEE Transactions on Magnetics*, 26, 3, 1160-1163, 1990.

[3] A. Mitra, D.C. Jiles, "Magnetic Barkhausen emissions in as-quenched Fe-Si-B amorphous alloy", *Journal of Magnetism and Magnetic Materials*, 168, 1-2, 169-176, 1997.

[4] C. Gatelier-Rothea, J. Chicois, R. Fougeres, P. Fleischmann, "Characterization of pure iron and (130 p.p.m.) carbon-iron binary alloy by Barkhausen noise measurements: study of the influence of stress and microstructure", *Acta Materialia*, 46, 14, 4873-4882, 1998.

[5] J. Anglada-Rivera, L.R. Padovese, J. Capo-Sanchez, "Magnetic Barkhausen Noise and hysteresis loop in commercial carbon steel: influence of applied tensile stress and grain size", *Journal of Magnetism and Magnetic Materials*, 231, 299-306, 2001.

[6] A. Martínez-de-Guerenu, K. Gurruchaga, F. Arizti, "Use of Magnetic Techniques for Characterisation of the Microstructure Evolution during the Annealing of Low Carbon Steels", *9th European Conference on Non-Destructive Testing (ECNDT)*, Berlin (Germany), 25-29 September, 2006. This proceedings.

[7] A.J. Birkett, W.D. Corner, B.K. Tanner, S.M. Thompson, "Influence of plastic deformation on Barkhausen power spectra in steels", *Journal of Applied Physics*, 22, 1240-1242, 1989.

[8] M. Zergoug, N. Boucherrou, A. Haddad, A. Benchaala, B. Moulti, H. Tahraoui, F. Sellidj, A. Hammouda, "Thermally affected characterization region by Barkhausen noise", *Ultrasonics*, 37, 703-707, 2000.

[9] B. Zhu, M.J. Johnson, C.C.H. Lo, D.C. Jiles, "Multifunctional Magnetic Barkhausen Emission Measurement System", *IEEE Transactions on Magnetics*, 37, 3, 1095-1099, 2001.

[10] L. Storm, C. Heiden, W. Grosse-Nobis, "The Power Spectrum of the Barkhausen Noise of Grain-Oriented Three-Percent Silicon Iron", *IEEE Transactions on Magnetics*, 2, 3, 434-438, 1966.

[11] H. Bittel, "Noise of Ferromagnetic Materials", *IEEE Transactions on Magnetics*, 5, 3, 359-365, 1969.

[12] N.J. Wiegman, R. Stege, "Barkhausen effect in magnetic thin films: general behaviour and stationarity along the hysteresis loop", *Journal of Applied Physics* ,16, 167-174, 1978.

[13] L. B. Magalas, "Application of the wavelet transform in mechanical spectroscopy and in Barkhausen noise analysis", *Journal of Alloys and Compounds*, 310, 269–275, 2000.

[14] A. Castelruiz, A. Martínez-de-Guerenu, K. Gurruchaga, F. Arizti, "Effect of the quantisation of the magnetising signal on magnetic Barkhausen noise measurements", *6th European Conference on Magnetic Sensors and Actuators*, Bilbao (Spain), 3-5 July, 2006.

[15] J.G. Proakis and D.G. Manolakis, "Introduction to Digital Signal Processing", *Macmillan Publishing Company*, New York, 1988.

[16] A. Martínez-de-Guerenu, F. Arizti, M. Díaz-Fuentes, I. Gutiérrez, "Recovery during annealing in a cold rolled low carbon steel. Part I: Kinetics and microstructural characterization", *Acta Materialia*, 52, 3657-3664, 2004.

[17] D.C. Jiles, "Dynamics of domain magnetization and the Barkhausen effect", *Czechoslovak Journal Of Physics*, 50, 8, 893-988, 2000.

[18] A. Martínez-de-Guerenu, .A. Galarza, A. Crespo, I. Leunda, F. Arizti, "Application of Barkhausen Noise Techniques to the Characterisation of Recovery and Recrystallization in Cold Rolled Low Carbon Steel", Proceedings of the *5th International Conference on Barkhausen Noise and Micromagnetic Testing (ICBM)*, pp. 59-70, Petten (The Netherlands), 2-3 June, 2005.